Original Paper

Glasses for the preparation of gradient index lenses in the $Na_2O-Al_2O_3-B_2O_3-SiO_2$ system – hydrolytic durability, thermal and optical properties

Sandra Hornschuh and Christian Rüssel
Otto-Schott-Institut für Glaschemie, Friedrich-Schiller-Universität Jena, Jena (Germany)

Bernhard Messerschmidt, Torsten Possner and Ulf Possner
GRINTECH GmbH, Jena (Germany)

Glasses in the system $Na_2O-Al_2O_3-B_2O_3-SiO_2$ were melted from the raw materials and studied with respect to their chemical durability, their crystal growth velocities, their refractive index and dispersion, their glass transition temperature and their thermal expansion coefficient. With increasing Na_2O concentration, the crystal growth velocity increases and the chemical durability decreases. Equimolar substitution of B_2O_3 for SiO_2 results in a decrease in both the chemical durability and in crystal growth velocities. Equimolar substitution of Al_2O_3 for SiO_2 leads to increasing chemical durability and decreasing crystal growth velocities. Optimum glass compositions to produce gradient index lenses should possess B_2O_3 concentrations of around 12.5 to 15 mol% and molar Al_2O_3 concentrations some percent larger than the Na_2O concentration. In these glasses, nonbridging oxygen does not occur.

1. Introduction

Up to now, most of the gradient index lenses produced worldwide are based on thallium containing glasses possessing a large thallium concentration in the middle and a smaller one in the outer part [1 and 2]. Due to the fact that thallium is extremely hazardous, great efforts to replace this component by environmentally safe compositions are made. Here, the first candidate which gives rise to large changes in the refractive index is silver. For that purpose, glasses in the system $Na_2O-Al_2O_3-B_2O_3-SiO_2$ with alkali concentrations $\geq$ 20 mol% Na_2O are already industrially used for the preparation of nonhazardous gradient index microlenses [3 to 8]. After preparing a glass rod possessing a diameter in the range of 1 to 3 mm, as a first step, an ion exchange in a salt melt containing $AgNO_3$ is carried out. Here, in the whole volume, around 90 % of the molar Na_2O concentration of the respective glass is exchanged for Ag_2O. The second step is an ion exchange of the Ag_2O containing glass in an $NaNO_3$ containing melt. Here, the ion exchange is interrupted, when the required concentration profile is achieved [9 to 13]. According to the demands on gradient index lenses, a parabolic profile is required, where the refractive index in the middle of the rod is larger (Ag_2O concentration larger) than in the outer part of the rod (Ag_2O concentration close to zero).

Received 22 April 2004.
Presented in German at: 78th Annual Meeting of the German Society of Glass Technology (DGG) in Nürnberg on 9 June 2004.

One of the main problems associated with the preparation procedure is the tendency of Ag_2O containing glasses to be reduced at elevated temperatures [14 to 16]. This effect may cause a yellow to black coloration, depending on the concentration of metallic silver in the glasses. This strongly limits the possible application of the as produced gradient index lenses, especially with respect to the wavelengths of light. It has been shown that the effect is small (light yellow coloration) if the glass used does not contain nonbridging oxygens [17 and 18]. For that purpose glasses in the system $Na_2O-Al_2O_3-B_2O_3-SiO_2$ have been developed [19]. For the preparation of gradient index microlenses, at first rods of the respective glass have to be prepared. This is usually done by drawing at temperatures in the range of 800 to 900 °C. Here, nucleation and crystallization of the respective glass has to be avoided. Other important physical properties of the glasses are the refractive index, the dispersion, the density and the viscosity. This paper provides a study of the dependence of these properties, including the crystal growth velocities, on the composition of the glasses. The silver diffusivity, its relation to the ionic conductivity of the glass, and the optical transmission as an effect of the glass composition will be reported in a separate paper.

2. Experimental procedure

The glasses were prepared from reagent grade $B(OH)_3$, $Al(OH)_3$, Na_2CO_3 and SiO_2 (quartz) in 300 g batches. They

Table 1. Chemical composition (concentrations in mol%) of the glasses studied

sample	Na_2O	Al_2O_3	B_2O_3	SiO_2
A	20	22.5	12.5	45
B	25	25	12.5	37.5
C	25	25	15	35
D	25	25	17.5	32.5
E	25	25	20	30
F	25	27.5	12.5	35
G	25	30	12.5	32.5
H	30	30	10	30
I	30	30	12.5	27.5
K	30	30	15	25
L	30	30	20	20
M	30	32.5	15	22.5
N	30	35	15	20

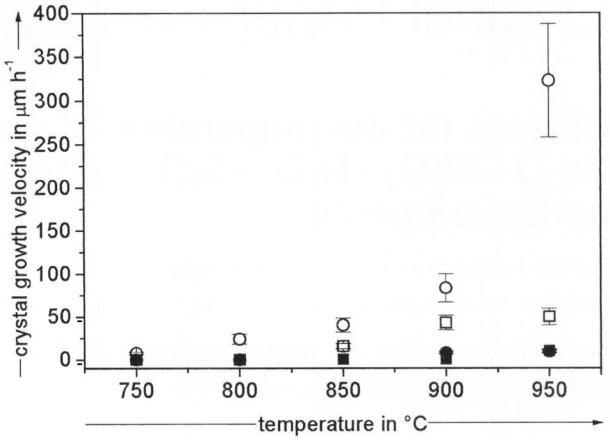

Figure 1. Crystal growth velocities of samples ○: B, ●: C, □: D, and ■: E as a function of the temperature.

were melted in platinum crucibles at a maximum temperature of 1500 °C in a furnace with $MoSi_2$ heating elements. The melts were cast on a graphite mould preheated to 500 °C, given to a muffle furnace with a temperature of 600 °C and then allowed to cool to room temperature.

The densities were measured with a helium pycnometer (Accupyc 1330, Micromeritics). Refractive indices were measured at the wavelengths 435.84 nm (n_g), 479.98 nm ($n_{F'}$), 546.06 nm (n_e), 587.56 nm (n_d) and 643.83 nm (n_c) using a Pulfrich refractometer (PRZ, Zeiss, Jena (Germany)) and samples with a rectangular angle. Abbe numbers were calculated by $v_e = (n_e-1)/(n_{F'}-n_c)$. The glass transformation temperature and the thermal expansion coefficient were measured dilatometrically (dilatometer 402 ES, Netzsch, (Germany)), using a heating rate of 5 K/min. Crystalline phases were detected by X-ray diffraction (Siemens D 5000, Siemens, München (Germany)). Crystal growth velocities were determined by light microscopy. Samples with a thickness of 3 mm were tempered at temperatures in the range from 700 to 950 °C, subsequently polished at both sides and then studied by light microscopy. The hydrolytic durability was determined according to DIN/ISO 719 [20].

3. Results

In table 1, the chemical compositions of all samples studied are summarized. Figures 1 to 3 show crystal growth velocities of all samples studied. In figure 1, samples with 25 mol% Na_2O and 25 mol% Al_2O_3 are shown. Here, the B_2O_3 concentration was varied between 12.5 and 20 mol%. In all cases, the crystal growth velocity increases with increasing temperature. In sample B, that with the smallest B_2O_3 concentration (12.5 mol%), the crystal growth velocity is 7 µm · h^{-1} at 750 °C and steadily increases to 324 µm · h^{-1} at 950 °C. Sample D has a larger B_2O_3 concentration (17.5 mol%), and crystallization could not be detected at temperatures in the range of 700 to 800 °C. At 850 °C, the crystal growth velocity is 15 µm · h^{-1}. At 900 and 950 °C, values of 43 and 50 µm · h^{-1} were respectively determined. In sample E, crystallization could not be detected at temperatures < 950 °C. It can be concluded that in the composition range shown in figure 1, the crystal growth velocity decreases with increasing B_2O_3/SiO_2 ratio. In figure 2, crystal growth velocities of samples with 30 mol% Na_2O and 30 mol% Al_2O_3 are shown. By analogy to figure 1, the B_2O_3 concentration was varied, here between 10 and 20 mol%. At a B_2O_3 concentration of 10 mol% (sample H), the crystal growth velocity is largest, 30 and 738 µm · h^{-1} at 750 and 950 °C, respectively. In sample I (B_2O_3 concentration: 12.5 mol%), the crystal growth velocities were smaller than in sample H in the entire temperature range studied. In samples K and L, crystallization could not be detected up to temperatures of 800 and 900 °C, respectively. It can be stated that by analogy to figure 1, also at the compositions shown in figure 2, increasing B_2O_3/SiO_2 ratios lead to decreasing crystal growth velocities. The crystal growth velocity increases in the entire temperature range studied. Figure 3 shows crystal growth velocities of samples A, F and M. They all exhibit Al_2O_3 concentrations 2.5 mol% larger than the respective Na_2O concentrations.

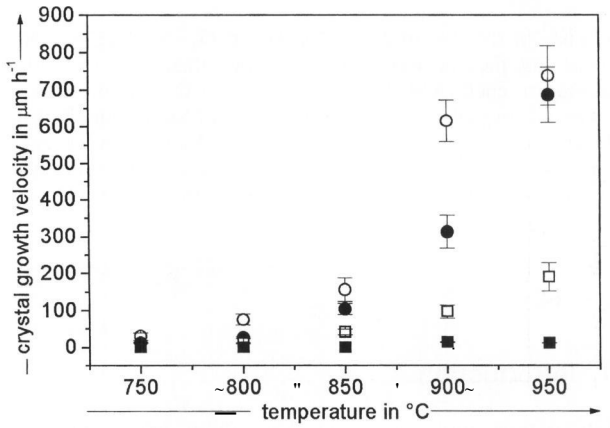

Figure 2. Crystal growth velocities of samples ○: H, ●: I, □: K, and ■: L as a function of the temperature.

Whereas in sample A crystallization was not detected at temperatures ≥ 950 °C, in samples F and M the lowest temperatures at which crystals were detected after temper-

Table 2. Density, refractive index n_e, Abbe number v_e, chemical solubility, glass transition temperature T_g, and linear thermal coefficient α of the glass samples studied

sample	density in g cm^{-3}	n_e	v_e	solubility in ml HCl	T_g in °C	$\alpha_{100\text{ to }300\,°C}$ in 10^{-7} K^{-1}
A	2.408	1.509	59.01 ± 0.1	0.42 ± 0.03	569	83
B	2.444	1.512	57.1 ± 3.2	2.03 ± 0.12	569	106
C	2.418	1.512	57.5 ± 3.2	2.82 ± 0.06	535	102
D	2.406	1.511	56.6 ± 3.1	4.17 ± 0.08	526	104
E	2.393	1.510	57.5 ± 0.1	3.68 ± 0.08	510	97
F	2.451	1.516	56.5 ± 0.6	2.50 ± 0.05	594	108
G	2.447	1.518	56.3 ± 0.6	1.08 ± 0.03	590	87
H	2.480	1.521	54.3 ± 0.6	5.42 ± 0.10	600	126
I	2.463	1.520	54.8 ± 0.6	7.90 ± 0.05	567	125
K	2.451	1.519	54.8 ± 0.1	32.30 ± 0.30	561	126
L	2.411	1.516	55.7 ± 0.6	42.30 ± 4.60	520	117
M	2.463	1.523	54.4 ± 0.3	11.20 ± 0.70	574	107
N	2.462	1.523	55.4 ± 0.6	18.48 ± 0.98	583	100

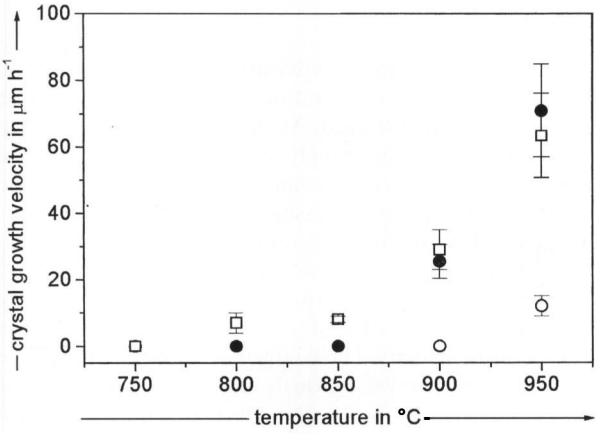

Figure 3. Crystal growth velocities of samples ○: A, ●: F, and □: M as a function of the temperature.

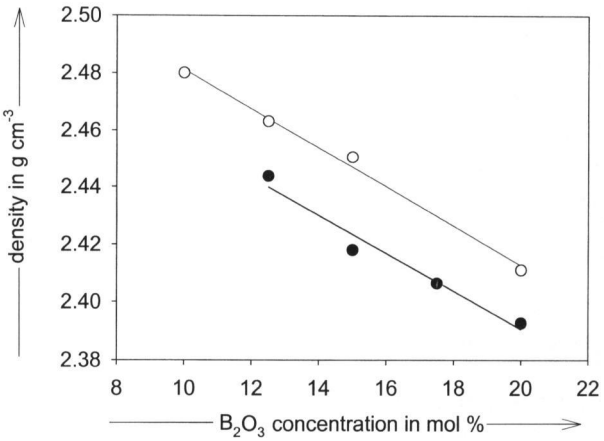

Figure 4. Density as a function of the boron oxide concentration for samples with $[Al_2O_3] = [Na_2O]$; ●: 25 mol% Al_2O_3, ○: 30 mol% Al_2O_3.

ing were 900 and 800 °C, respectively. The crystal growth velocities were smallest in the sample with 20 mol% Na_2O. Generally, crystal growth velocities were smaller than in samples with $[Na_2O] = [Al_2O_3]$ (compare figures 1 and 2). Thus, an excess of Al_2O_3 hinders the crystal growth in the composition range studied. Samples G and N exhibit Al_2O_3 concentrations 5 mol% larger than the respective Na_2O concentrations. Here, a further decrease in the crystal growth velocity was observed. In samples A and L, a crystalline phase could not be detected by X-ray diffraction, all other crystallized samples exhibited $NaAlSiO_4$ (JCPDS no. 35-0424 [21]) as crystalline phase.

Table 2 summarizes density, refractive index, n_e, Abbe number, v_e, value of the chemical durability, the glass transition temperature, T_g, and the thermal expansion coefficient, α, for all glass samples studied. The densities vary between 2.393 and 2.480 g · cm^{-3}. The densities increase with increasing Al_2O_3 concentration and decrease if the B_2O_3 concentrations are larger. In figure 4, the effect on the boron concentration is shown for samples with $[Na_2O] = [Al_2O_3]$. For both Na_2O concentrations, 25 and 30 mol%, a linear decrease with increasing B_2O_3 concentration is observed. Samples with a larger Na_2O (and Al_2O_3) concentration exhibit larger densities. The equimolar replacement of 2.5 mol% SiO_2 with Al_2O_3 leads to an increase in the density (not shown in figure 4). If 5 mol% SiO_2 are replaced with Al_2O_3, the obtained densities are smaller again. Refractive indices are all in the range of 1.509 to 1.523, a slight increase with increasing Al_2O_3 as well as with decreasing B_2O_3 concentration is observed. The Abbe number increases slightly with increasing B_2O_3 and decreasing Al_2O_3 concentrations. Figure 5 shows the chemical solubility for all samples studied with $[Na_2O] = [Al_2O_3]$. It is seen that the solubility increases with increasing B_2O_3 concentration. For 30 mol% Al_2O_3 (and Na_2O), the values are up to one order of magnitude larger than for 25 mol% Na_2O. If 2.5 mol% SiO_2 are replaced by an equimolar concentration of Al_2O_3, the chemical solubility of the series with 30 mol% Na_2O decreases, and the corresponding ml HCl drop from 42 to 11.2. If 5 mol% SiO_2 are substituted, the chemical solubility increases again. It can be stated that within the concen-

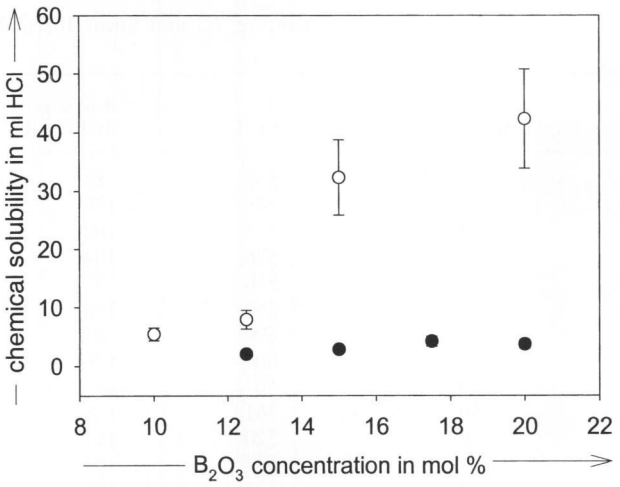

Figure 5. Chemical solubility as a function of the boron oxide concentration for samples with $[Al_2O_3] = [Na_2O]$; ●: 25 mol% Al_2O_3, ○: 30 mol% Al_2O_3.

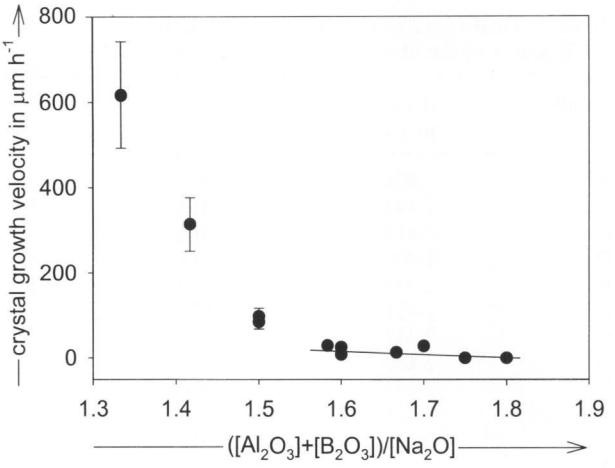

Figure 7. Crystal growth velocities at 900 °C as a function of the $([Al_2O_3] + [B_2O_3])/[Na_2O]$ ratio. Line: regression line (only for $([Al_2O_3] + [B_2O_3])/[Na_2O] > 1.5$).

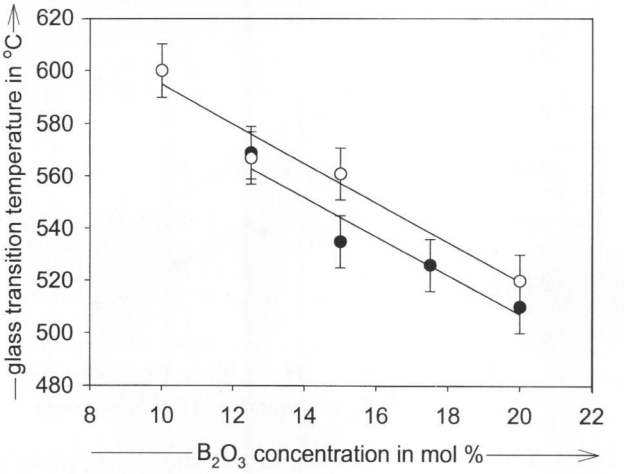

Figure 6. Glass transition temperature, T_g, as a function of the boron oxide concentration for samples with $[Al_2O_3] = [Na_2O]$; ●: 25 mol% Al_2O_3, ○: 30 mol% Al_2O_3.

tration range studied, the chemical solubility increases with increasing Na_2O and B_2O_3 concentrations. If $[Al_2O_3]$ is slightly larger than $[Na_2O]$, a decrease in the chemical solubility is observed.

Figure 6 presents the glass transition temperatures as a function of the B_2O_3 concentration for samples with $[Na_2O] = [Al_2O_3]$. For both Na_2O concentrations (25 and 30 mol%), T_g decreases linearly within the limits of error. The regression line attributed to the larger Na_2O (and Al_2O_3) concentration runs parallel to that calculated for the smaller Na_2O concentration and is shifted by 12 K to larger temperatures. Replacement of SiO_2 by Al_2O_3 results in larger glass transition temperatures.

4. Discussion

In order to draw rods for the production of gradient index lenses, the glass has to be stable towards devitrification at temperatures attributed to viscosities of around 10^6 dPa s. This corresponds to temperatures in the range of 800 to 900 °C in the system studied. As shown in figures 1 to 3, the crystal growth velocity strongly depends on the temperature supplied and the chemical composition used. Whereas the crystal growth velocity increases steadily with the temperature supplied (in the range studied), the crystal growth velocities increase with increasing Na_2O concentration and decreasing B_2O_3 concentration. Replacement of SiO_2 by equimolar quantities of Al_2O_3 results in a decrease of the crystal growth velocity. These effects are illustrated in figure 7 by a plot of the crystal growth velocity at 900 °C against the ratio $([Al_2O_3] + [B_2O_3])/[Na_2O]$. If this ratio decreases, first a linear increase of the crystal growth velocity is observed. If, however, the ratio $([Al_2O_3] + [B_2O_3])/[Na_2O]$ is smaller than 1.5, a drastic increase of the crystal growth velocity occurs. Since, as shown in figure 6, T_g decreases with increasing B_2O_3 concentration, also the viscosity decreases. This means that crystal growth velocities related to a constant viscosity (not temperature) decrease with increasing B_2O_3 concentration even more pronounced than shown in figure 7. The reason for this effect first of all should be seen in the increasing deviation of the glass composition from that of the crystalline phase formed during devitrification ($NaAlSiO_4$). In the range studied, the chemical composition possesses only a minor effect on the density, refractive index and Abbe number. The equimolar substitution of B_2O_3 for SiO_2 results in smaller densities, which is not surprising regarding the smaller atomic weight. If both Na_2O and Al_2O_3 are substituted for SiO_2, the density increases due to a more compact glass structure. It should be noted that refractive indices and Abbe numbers are in the range suitable for the production of gradient index lenses. Concerning the structure of the studied glasses, first sample B should be considered. Here, both the molar Na_2O and the Al_2O_3 concentrations are 25 %. The other melt components, B_2O_3 and SiO_2 (molar ratio B_2O_3/SiO_2 is 1:3) are network formers, the sum of their concentrations is another 50 %. An idealized glass structure might consist of AlO_4^- tetrahedra whose formally negative charge is compensated by Na^+ cations. Besides, SiO_4 tetrahedra occur and all boron

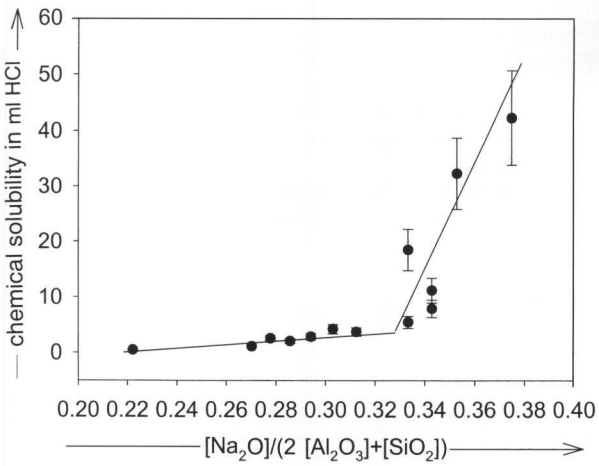

Figure 8. Chemical solubility as a function of the ratio $[Na_2O]/(2[Al_2O_3] + [SiO_2])$.

is in threefold coordination. The real glass structure should be somewhat different: the main part of the alumina occurs as AlO_4^- tetrahedra, besides some boron also exists in fourfold coordination, i.e. as BO_4^- tetrahedra. Since the total concentration of MO_4^- tetrahedra ($[AlO_4^-] + [BO_4^-]$) must be equal to the Na^+ concentration, alumina also occurs in sixfold coordination. In the described structure, nonbridging oxygen does not occur. If now, both the Al_2O_3 and the Na_2O concentration increase, the structure does not notably change, alumina predominantly occurs as AlO_4^- tetrahedra whose charge is compensated by Na^+. If however SiO_2 is replaced with Al_2O_3, excess alumina can no longer be incorporated in tetrahedral coordination, but must occur in octahedral coordination or as triclusters [22]. The substitution of B_2O_3 for SiO_2 cannot lead to the incorporation of B_2O_3 in tetrahedral concentration [23]. Since in all compositions studied, the alumina concentration is equal or larger than the Na_2O concentration, excess B_2O_3 must be incorporated in threefold coordination. According to the literature this leads to a decrease in the glass transition temperature, and also to an increase in the chemical solubility (see figure 5). However, the effect of the glass structure on the chemical solubility is more complex. Figure 8 presents the chemical solubility (ml HCl) as a function of the ratio $[Na_2O]/(2[Al_2O_3] + [SiO_2])$. It is observed that for ratios < 0.34, the solubility increases steadily and within the limits of errors linearly. If the ratio is larger than 0.34, a drastic increase, however, is observed. The increase in the chemical solubility with increasing Na_2O concentration is as expected, while the increase in the silica and, in the most cases, in the alumina concentration leads to a decrease in the chemical solubility.

In the following, glasses with 25 and 30 mol% Na_2O should be discussed separately. In the composition series with 25 mol% Na_2O, the tendency to crystallization can be suppressed by substituting equimolar concentrations of B_2O_3 or Al_2O_3 for SiO_2. While the substitution of B_2O_3 leads to a decrease in the chemical solubility, this does not occur in the case of Al_2O_3. Here, small chemical solubility and small crystal growth velocities can be achieved for the samples F and G. The compositions with 30 mol% Na_2O should enable the preparation of lenses with a larger gradient in the refractive index. However, the larger Na_2O concentrations lead to both, larger chemical solubility and larger crystal growth velocities. The tendency to crystallization can widely be suppressed by the substitution of B_2O_3 for SiO_2. However, this also leads to a further increase in the chemical solubility. The substitution of equimolar Al_2O_3 concentrations for SiO_2, however, leads to a decrease in the chemical solubility and to a decrease in the crystal growth velocity. Therefore, optimum glass compositions should possess B_2O_3 concentrations in the range of 12.5 to 15 mol% and Al_2O_3 concentrations a few mole percent larger than the Na_2O concentrations. Glasses in this composition range should have crystal growth velocities small enough for the rod drawing process. The chemical durability should be sufficient for most applications.

5. References

[1] Kaps, C.: Peculiarities of alkali thallium ion-exchange in oxide glasses – aspects of thermodynamics and kinetics for generation of optical wave-guide layers. J. Non-Cryst. Solids **123** (1990) pp. 315–320.

[2] Jackel, J.: High-delta-n optical wave-guides in $LiBO_3$–thallium-lithium ion-exchange. Appl. Phys. Lett. **37** (1980) pp. 739–741.

[3] Feltz, A.; Popp, P.; Kaps, C. et al.: Optisches Glas mit hohen Kationendiffusionskoeffizienten. Germ. pat no. DE 3608967 A1. (18.03.1986.)

[4] Poßner, T.; Schreiter, G.; Müller, R.: Special glass for integrated and microoptics. Glastech. Ber. **64** (1991) pp. 185–190.

[5] Kaps, C; Feltz, A.; Göring, R. et al.: Verfahren zur Erzeugung großer Brechzahlunterschiede in kompakten Gläsern. Germ. pat. no. DD 269615 A1. (30.09.1985.)

[6] Yamsguchi, J.; Kittaka, S.: Graded index lens. Europ. pat. no. EP 1106586 A1. (01.12.2000.)

[7] Houde-Walter, S. N.; Inman, J. M.; Dent, A. J. et al.: Sodium and silver environments and ion-exchange processes in silicate and alumosilicate glasses. J. Phys. Chem. **97** (1993) pp. 9330–9336.

[8] Spierings, G.; Bommel, J. M.: Ag^+-Na^+ ion exchange in boroalumosilicat glasses. J. Non-Cryst. Solids **113** (1989) pp. 37–40.

[9] Messerschmidt, B.; Hsieh, C. H.; McIntyre, B. L. et al.: Ionic mobility in an ion exchanged silver-sodium boroaluminosilicate glass for micro-optics applications. J. Non-Cryst. Solids **217** (1997) pp. 264–271.

[10] Messerschmidt, B.; McIntyre, B. L.; Houde-Walter, S. N.: Desired concentration-dependent ion exchange for micro-optic lenses. Appl. Opt. **35** (1996) pp. 5670–5676.

[11] Ohmi, S.; Sakai, H.; Nakayama, S. et al.: Gradient-index rod lens made by double ion-exchange process. Appl. Opt. **27** (1988) pp. 496–499.

[12] Messerschmidt, B.; Possner, T.; Goering, R.: Colorless gradient index cylindrical lenses with high numerical apertures by silver-ion exchange. Appl. Opt. **34** (1995) pp. 7825–7830.

[13] Messerschmidt, B.; Possner, U.; Houde-Walter, S. N.: Fabrication tolerances and metrology requirements for ion-exchanged micro-optic lenses: What's good enough? Appl. Opt. **36** (1997) pp. 8145–8152.

[14] Araujo, R. J.: Colourless glasses containing ion-exchanged silver. Appl. Opt. **31** (1992) pp. 5221–5224.

[15] Dimitryuk, A. V.; Soloveva, N. D.; Timofeev, N. T.: The problem of silver atoms stabilization in glass. Glastech. Ber. Glass Sci. Technol. **68 C1** (1995) pp. 111–115.

[16] Araujo, R. J.: High silver borosilicate glasses. World pat. no. WO 02/14233 A1. (21.02.1002.)

[17] Inman, J. M.; Houde-Walter, S. N.; McIntyre, B. L. : Chemical structure and the mixed mobile ion effect in sil-

ver-for-sodium ion exchange in silicate glasses. J. Non-Cryst. Solids **194** (1996) pp. 85–92.
[18] Kaps, C.; Fliegel, W.: Sodium/silver ion exchange between a non-bridging oxygen-free boroaluminosilicate glass and nitrate melts. Glastech. Ber. **64** (1991) pp. 199–204.
[19] Popp, P.; Göring, R.; Feltz, A. et al.: Gläser zur Erzeugung ausgedehnter Brechzahlverteilungen hoher Transparenz. Germ. pat. no. DE 3803420 A1. (05.02.1988.).
[20] International standard DIN/ISO 719 (Dec. 1989): Wasserbeständigkeit von Glasgrieß bei 98 °C. Geneva: ISO 1989.
[21] Powder Diffraction File Card. International Centre for Diffraction Data (ICDD). Newton Square, PA. (Formerly: Joint Committee for Powder Diffraction Standards (JCPDS).)
[22] Engelhardt, G.; Nofz, M.; Forkel, K. et al.: Structural studies of calcium aluminosilicate glasses by high resolution solid state ^{29}Si and ^{27}Al magic angle spinning nuclear magnetic resonance. Phys. Chem. Glasses **26** (1985) pp. 157–165.
[23] Araujo, R. J.: Statistical mechanical model of boron coordination. J. Non-Cryst. Solids **42** (1980) pp. 209–230.
E604P003

Contact:

Prof. Dr. C. Rüssel
Otto-Schott-Institut für Glaschemie
Friedrich-Schiller-Universität Jena
Fraunhoferstr. 6
D-07743 Jena

E-mail: ccr@rz.uni-jena.de